



Synthesis, crystal structure and properties of a yttrium complex based on mixed functional ligands

Hongzhe Jin, Xiaoming Peng, Lei Guan*, Ying Wang & Xuejia Xiong
School of Petrochemical Engineering, Liaoning Shihua University, Fushun 113001
*E-mail: advcoord@163.com

Received 05 August 2020; revised and accepted 10 September 2020

A new yttrium complex, $[Y_2(H_2Dhbds)_3(phen)_2] \cdot [Y_2(H_2Dhbds)_2(H_2Thbs)(phen)_2]$ (**1**) (Na_2H_2Dhbds = 4,5-dihydroxy-1,3-benzenedisulfonic acid disodium salt; NaH_3Thbs = 2,3,5-trihydroxy-1-benzenesulfonic acid sodium salt), has been synthesized and structurally characterized. Complex **1** consists of two dinuclear structural units bridged by H_2Dhbds^{2-} and H_2Thbs^{2-} ligands, where phen molecules act as N, N-bidentate ligands, chelating Y atoms. The dinuclear structural units are connected by π - π stacking interactions between phen molecules, generating a one-dimensional chain structure. In addition, complex **1** exhibits the broad fluorescent emission band at 365 nm, which originates from intraligand charge transitions.

Keywords: Synthesis, Yttrium complex, Mixed functional ligand, π - π stacking interactions, Intraligand charge transition

Coordination complexes have received extensive attention in recent year, owing to their intriguing structures and potential applications in many fields, such as gas storage, sensing, photoluminescence, and catalysis¹⁻⁶. Because the structures of complexes have the great effect on their properties and functionalities, the organic ligands, acting as structure-directing building blocks, play the important roles in the functional complexes⁷⁻¹⁰. So far, the impressive progress of syntheses and applications of complexes has been made, however, it remains a significant challenge to design complex functional materials. Much effort has been devoted to design and decorate the building blocks in order to control the self-assembly for required products¹¹⁻¹⁴.

Recently, the utilization of organic ligands containing two different functional groups for the synthesis of coordination complexes has received increasing interest¹⁵⁻¹⁷. The number of functional groups, their coordination modes, charge and acidity have strong effects on the structures, chemical and physical properties of complexes¹⁸. Examples from reported work comprise the use of phosphonate-carboxylate, sulfonate-carboxylate, carboxylate-phenol ligands¹⁹⁻²¹. In contrast, not much attention has been paid to the multifunctional sulfonate-phenol ligands in these years, where sulfonate group with weak coordination ability can make its coordination mode more flexible and can easily form hydrogen

bonds with H-donor; phenol group is capable to bind to metal ions in the bridging and monodentate coordination modes^{22, 23}. These two groups can cooperate with each other and bind to metal ions, generating novel complex and more stabilized structure. H_2Dhbds^{2-} and H_2Thbs^{2-} ligands with sulfonate and phenol groups stationed on a phenyl central motif are expected to be effective building blocks for the construction of novel coordination complexes.

Homobinuclear metal complexes are of significant interest due to their structure-dependent properties, which are very useful for developing new molecule-based materials. The design of functional complexes of homobinuclear centers with diverse structures has been the subject of extensive investigations. This remarkable diversity is achieved by reasonable choice of their central metal ions. Especially for homobinuclear rare earth metal complexes, the sensitization of ligands to metal ions is effectively hindered, and the fluorescence emissions of the complexes are mainly attributed to intraligand charge transitions.

Here, we report a new yttrium coordination complex based on multifunctional sulfonate-phenol and phen mixed ligands, $[Y_2(H_2Dhbds)_3(phen)_2] \cdot [Y_2(H_2Dhbds)_2(H_2Thbs)(phen)_2]$, which is an unexpected complex possessing two dinuclear structural units bridging by H_2Dhbds^{2-} and H_2Thbs^{2-}

ligands. Furthermore, the thermal stability and fluorescence properties are also described.

Materials and Methods

All chemicals and solvents used for the experiment were purchased from Sinopharm Chemical Reagent Co., Ltd, which were analytical reagents and used without further purification. Crystal structure measurement was performed on a Bruker Smart Apex II CCD diffractometer. The FTIR spectrum was recorded on a Nicolet FTIR spectrometer using KBr pellets in the range of 4000-400 cm^{-1} . After removing lattice solvent molecules from the sample by heat treatment, elemental analysis of the sample was performed with an Elementar Vario EL analyzer, and thermogravimetric analysis was carried out on a 1100SF thermal analyzer at a heating rate of 10 $^{\circ}\text{C}\cdot\text{min}^{-1}$ under a nitrogen atmosphere. Photoluminescence analysis was performed on a Perkin Elemer LS55 fluorescence spectrometer.

Synthesis of complex 1

A mixture of $\text{Y}(\text{NO}_3)_3\cdot 6\text{H}_2\text{O}$ (0.038 g, 0.1 mmol), $\text{Na}_2\text{H}_2\text{Dhbd}$ s (0.031 g, 0.1 mmol), NaH_3Thbs (0.023 g, 0.1 mmol), phen (0.018 g, 0.1 mmol), ethanol (10 mL) and water (10 mL) was sealed in Teflon-lined autoclave and heated at 160 $^{\circ}\text{C}$ for 5 days, followed by slow cooling to room temperature. The pale yellow block crystals of complex 1 were isolated and washed with water (yield: ca. 52% based on $\text{Na}_2\text{H}_2\text{Dhbd}$ s). Elemental analysis of $\text{C}_{84}\text{H}_{56}\text{N}_8\text{O}_{46}\text{S}_{11}\text{Y}_4$: calcd. C 38.48; H 2.14 N 4.27%; found: C 38.57; H 2.30; N 4.33%. IR (KBr cm^{-1}): 3413($\nu_{\text{O-H}}$), 1598($\nu_{\text{C=C}}$), 1520($\nu_{\text{C=C}}$), 1540($\nu_{\text{C=C}}$), 1470($\nu_{\text{C=N}}$), 1422($\nu_{\text{C=N}}$), 1275($\nu_{\text{C-O}}$), 1237($\nu_{\text{as S-O}}$), 1138($\nu_{\text{S-O}}$), 1097($\nu_{\text{S-O}}$), 1019($\nu_{\text{S-O}}$), 847($\gamma_{\text{C-H}}$), 775($\gamma_{\text{C-H}}$), 717($\gamma_{\text{C-H}}$), 655($\gamma_{\text{C-H}}$), 610($\delta_{\text{S-O}}$).

X-ray crystallographic measurement

The X-ray single crystal data collection for the complex 1 was performed on a Bruker Smart Apex II CCD diffractometer equipped with graphite monochromated MoK_α radiation ($\lambda = 0.71073 \text{ \AA}$) at 293 K. After absorption correction, the structure was solved by direct method and refined by a full-matrix least squares method on F^2 using SHELXT 2018 and SHELXL 2018 programs^{24, 25}. The hydrogen atoms were generated geometrically and treated by a mixture of independent and constrained refinement. The free solvent molecules are disordered, so they are removed from the structure. The crystallographic data are

summarized in Table 1, while selected bond lengths and angles are given in Table 2. The hydrogen bonding interactions in complex 1 were not observed.

Table 1 — Crystal data and structure refinement for complex 1

Chemical formula	$\text{C}_{84}\text{H}_{56}\text{N}_8\text{O}_{46}\text{S}_{11}\text{Y}_4$
M_r	2621.66
Crystal system, space group	Triclinic, $P-1$
Temperature (K)	293
a, b, c (\AA)	15.073(2), 22.000(3), 35.726(5)
α, β, γ ($^{\circ}$)	95.032(2), 91.122(3), 95.031(3)
V (\AA^3)	11751 (3)
Z	2
μ (mm^{-1})	1.12
Crystal size (mm)	$0.25 \times 0.22 \times 0.19$
$T_{\text{min}}, T_{\text{max}}$	0.767, 0.816
No. of measured, independent and observed [$I > 2\sigma(I)$] reflections	65497, 41128, 13293
R_{int}	0.068
$(\sin \theta/\lambda)_{\text{max}}$ (\AA^{-1})	0.595
$R[F^2 > 2\sigma(F^2)], wR(F^2), S$	0.094, 0.207, 1.15
No. of reflections	41128
No. of parameters	1261
No. of restraints	144
$\Delta\rho_{\text{max}}, \Delta\rho_{\text{min}}$ (e \AA^{-3})	0.70, -1.27

Table 2 — Selected Bond Lengths (\AA) and Bond Angles ($^{\circ}$) for complex 1

N1—Y3	2.493(6)	O16—Y3	2.304(5)
N2—Y3	2.562(7)	O17—Y2	2.247(6)
N3—Y2	2.483(8)	O18—Y3	2.338(5)
N4—Y2	2.563(6)	O24—Y4	2.259(6)
N5—Y1	2.521(6)	O25—Y4	2.248(5)
N6—Y1	2.471(7)	O25—Y1	2.273(5)
N7—Y4	2.525(7)	O26—Y1	2.380(6)
N8—Y4	2.495(7)	O32—Y4	2.345(6)
O1—Y3	2.369(5)	O35—Y4	2.304(5)
O1—Y2	2.371(5)	O35—Y1	2.352(5)
O2—Y2	2.437(5)	O36—Y1	2.322(5)
O8—Y3	2.317(6)	O40—Y4	2.433(6)
O9—Y3	2.329(6)	O41—Y4	2.351(6)
O10—Y3	2.316(5)	O41—Y1	2.383(6)
O10—Y2	2.337(5)	O42—Y1	2.321(6)
O11—Y2	2.314(5)	Y1—Y4	3.5218(13)
O16—Y2	2.293(5)	Y2—Y3	3.5267(12)
O25—Y1—O42	119.9(2)	O16—Y3—O8	119.4(2)
O25—Y1—O36	135.02(17)	O16—Y3—O10	69.37(18)
O42—Y1—O36	84.91(19)	O8—Y3—O10	136.50(19)
O25—Y1—O35	69.08(18)	O16—Y3—O9	135.81(18)
O42—Y1—O35	134.84(19)	O8—Y3—O9	83.6(2)
O36—Y1—O35	67.36(17)	O10—Y3—O9	68.7(2)
O25—Y1—O26	74.31(18)	O16—Y3—O18	72.64(17)
O42—Y1—O26	82.2(2)	O8—Y3—O18	82.03(19)

(Contd.)

Table 2 — Selected Bond Lengths (Å) and Bond Angles (°) for complex 1 (Contd.)

O36—Y1—O26	150.15(17)	O10—Y3—O18	136.02(18)
O35—Y1—O26	137.63(18)	O9—Y3—O18	151.43(18)
O25—Y1—O41	66.2(2)	O16—Y3—O1	67.29(18)
O42—Y1—O41	75.9(2)	O8—Y3—O1	74.92(17)
O36—Y1—O41	87.58(19)	O10—Y3—O1	70.46(18)
O35—Y1—O41	68.28(19)	O9—Y3—O1	86.01(18)
O26—Y1—O41	114.9(2)	O18—Y3—O1	113.63(18)
O25—Y1—N6	83.6(2)	O16—Y3—N1	139.7(2)
O42—Y1—N6	142.3(2)	O8—Y3—N1	78.4(2)
O36—Y1—N6	98.6(2)	O10—Y3—N1	124.5(2)
O35—Y1—N6	79.1(2)	O9—Y3—N1	78.0(2)
O26—Y1—N6	76.3(2)	O18—Y3—N1	75.02(19)
O41—Y1—N6	141.4(2)	O1—Y3—N1	150.2(2)
O25—Y1—N5	139.5(2)	O16—Y3—N2	84.2(2)
O42—Y1—N5	79.1(2)	O8—Y3—N2	141.9(2)
O36—Y1—N5	77.57(19)	O10—Y3—N2	77.7(2)
O35—Y1—N5	124.8(2)	O9—Y3—N2	100.0(2)
O26—Y1—N5	73.6(2)	O18—Y3—N2	77.2(2)
O41—Y1—N5	152.0(2)	O1—Y3—N2	142.9(2)
N6—Y1—N5	65.3(2)	N1—Y3—N2	65.6(2)
O25—Y1—Y4	38.58(13)	O16—Y3—Y2	39.79(12)
O42—Y1—Y4	116.89(14)	O8—Y3—Y2	116.28(13)
O36—Y1—Y4	97.80(11)	O10—Y3—Y2	40.93(14)
O35—Y1—Y4	40.34(12)	O9—Y3—Y2	97.10(13)
O26—Y1—Y4	112.05(13)	O18—Y3—Y2	111.40(12)
O41—Y1—Y4	41.58(14)	O1—Y3—Y2	41.94(12)
N6—Y1—Y4	99.88(15)	N1—Y3—Y2	164.20(17)
N5—Y1—Y4	163.16(17)	N2—Y3—Y2	101.04(17)
O17—Y2—O16	69.95(18)	O25—Y4—O24	70.5(2)
O17—Y2—O11	81.3(2)	O25—Y4—O35	70.37(19)
O16—Y2—O11	130.8(2)	O24—Y4—O35	99.30(19)
O17—Y2—O10	98.3(2)	O25—Y4—O32	129.8(2)
O16—Y2—O10	69.19(18)	O24—Y4—O32	80.2(2)
O11—Y2—O10	76.84(18)	O35—Y4—O32	75.5(2)
O17—Y2—O1	137.21(18)	O25—Y4—O41	67.1(2)
O16—Y2—O1	67.43(17)	O24—Y4—O41	137.5(2)
O11—Y2—O1	131.22(19)	O35—Y4—O41	69.6(2)
O10—Y2—O1	70.08(18)	O32—Y4—O41	131.3(2)
O17—Y2—O2	156.69(19)	O25—Y4—O40	130.3(2)
O16—Y2—O2	131.45(18)	O24—Y4—O40	157.5(2)
O11—Y2—O2	76.7(2)	O35—Y4—O40	82.96(18)
O10—Y2—O2	84.32(18)	O32—Y4—O40	78.7(2)
O1—Y2—O2	65.47(17)	O41—Y4—O40	64.4(2)
O17—Y2—N3	88.2(2)	O25—Y4—N8	78.1(2)
O16—Y2—N3	77.8(2)	O24—Y4—N8	88.4(2)
O11—Y2—N3	141.6(2)	O35—Y4—N8	142.6(2)
O10—Y2—N3	141.5(2)	O32—Y4—N8	141.8(2)
O1—Y2—N3	79.4(2)	O41—Y4—N8	80.0(2)
O2—Y2—N3	104.21(19)	O40—Y4—N8	103.5(2)
O17—Y2—N4	87.6(2)	O25—Y4—N7	136.6(3)
O16—Y2—N4	136.7(2)	O24—Y4—N7	86.9(2)

(Contd.)

Table 2 — Selected Bond Lengths (Å) and Bond Angles (°) for complex 1 (Contd.)

O11—Y2—N4	78.1(2)	O35—Y4—N7	152.0(2)
O10—Y2—N4	153.0(2)	O32—Y4—N7	78.7(2)
O1—Y2—N4	121.8(2)	O41—Y4—N7	122.6(2)
O2—Y2—N4	80.39(19)	O40—Y4—N7	81.4(2)
N3—Y2—N4	64.6(2)	N8—Y4—N7	64.3(2)
O17—Y2—Y3	102.78(13)	O25—Y4—Y1	39.09(14)
O16—Y2—Y3	40.01(13)	O24—Y4—Y1	102.23(14)
O11—Y2—Y3	117.32(13)	O35—Y4—Y1	41.37(13)
O10—Y2—Y3	40.49(13)	O32—Y4—Y1	116.74(15)
O1—Y2—Y3	41.91(11)	O41—Y4—Y1	42.28(14)
O2—Y2—Y3	94.22(12)	O40—Y4—Y1	94.26(13)
N3—Y2—Y3	101.03(16)	N8—Y4—Y1	101.21(15)
N4—Y2—Y3	162.30(18)	N7—Y4—Y1	163.0(2)

Crystallographic data were deposited with the Cambridge Crystallographic Data Centre (CCDC 2017528). The data can be obtained free of charge via <http://www.ccdc.cam.ac.uk/conts/retrieving.html> or from the Cambridge Crystallographic Data Centre, 12 Union Road, Cambridge CB2 1EZ, UK; fax: (+44-1223-336-033); or e-mail: deposit@ccdc.cam.ac.uk.

Results and Discussion

Crystal structure of complex 1

Single crystal X-ray analysis revealed that complex **1** crystallized in the triclinic group *P*-1 (Table 1). The asymmetrical unit consists of four Y ions, five H₂Dhbds anions, one H₂Thbs anion and four coordinated phen molecules. Both meta-phenol groups of H₂Dhbds²⁻ and H₂Thbs²⁻ ligands were protonated to maintain the charge balance of complex **1** (Fig. 1). Complex **1** is composed of two dinuclear structural units. However, one difference between two dinuclear units is that one dinuclear structural unit contains three H₂Dhbds²⁻ linkers, the other has two H₂Dhbds²⁻ and one H₂Thbs²⁻ linkers. The eight-coordinate environment of each Y2 atom is completed by five phenol oxygen atoms from three H₂Dhbds²⁻ ligands, one sulfonate oxygen atom from H₂Dhbds²⁻ ligand, and two nitrogen atoms from one phen molecule. Each Y3 sits in an eight-coordinate environment composed of four phenol oxygen atoms from three H₂Dhbds²⁻ ligands, two sulfonate oxygen atoms from two H₂Dhbds²⁻ ligands, and two nitrogen atoms from one phen molecule. Y2 and Y3 atoms are all in distorted double capped triangular prism geometries (Fig. 2a). The coordination environment and geometries of Y4 and Y1 atoms are the same as those of Y2 and Y3 atoms, respectively (Fig. 2b). The neighboring Y2 and Y3 atoms are bridged by phenol

μ_2 -O1, O10 and O16 atoms, resulting in the formation of a dinuclear [Y2-O₃-Y3] unit with the Y...Y distance of 3.5267 Å (Fig. 3a). The additional three bridged phenol μ_2 -O25, O35 and O41 atoms are bonded to the neighbouring Y1 and Y4 ions through forming a dinuclear [Y1-O₃-Y4] unit, with the Y...Y distance of 3.5218 Å (Fig. 3b). The dinuclear structural units are cross-linked through the offset face-to-face π - π stacking interactions between neighbouring phen molecules with the centroid-to-centroid distances of 3.5728 Å and 3.6457 Å, thus a one-dimensional chain supramolecular structure is

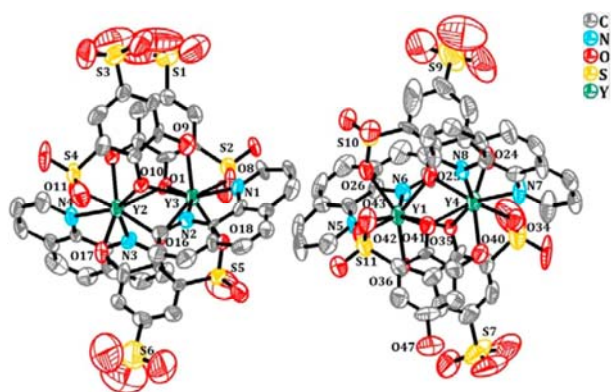


Fig. 1 — The molecular structure of complex **1**. The asymmetric structure unit of complex **1** with atomic labeling scheme. All hydrogen atoms are omitted for clarity

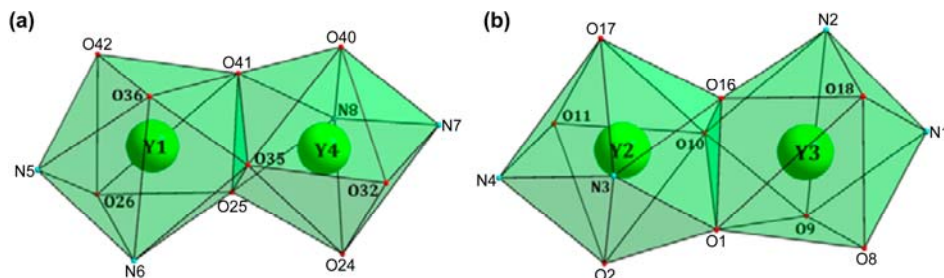


Fig. 2 — (a) Y1 and Y4 ions, (b) Y2 and Y3 ions exhibit distorted double capped triangular prism geometries, respectively

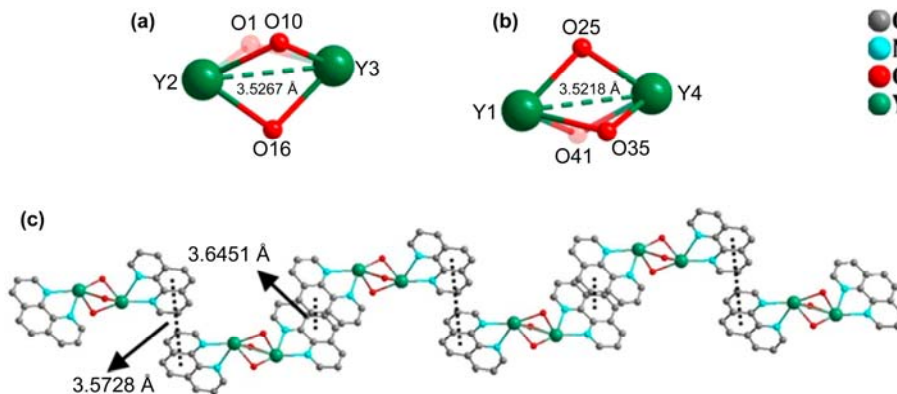


Fig. 3 — (a) [Y2-O₃-Y3] dinuclear structural unit, (b) [Y1-O₃-Y4] dinuclear structural unit, (c) A one-dimensional chain structure generated by the offset face-to-face π - π stacking interactions between neighbouring phen molecules of the dinuclear structural units

formed (Fig. 3c). The Y-O and Y-N bond lengths are in the range of 2.247(6) Å – 2.437(5) Å and 2.471(7) Å–2.563(6) Å (Table 2), respectively, which are comparable to the values in other reported Y complexes^{26, 27}. The H₂Dhbs²⁻ and H₂Thbs²⁻ ligands exhibit similar coordination modes, which bridge two Y ions through one monodentate sulfonate oxygen atom, one μ_1 -phenol oxygen atom and one bridging phenol oxygen atom, leaving other sulfonate and phenol groups uncoordinated, respectively (Fig. 4).

Previous studies have indicated that the auxiliary bridging ligands, such as 4,4'-bipy and 1,3-di(4-pyridyl)propane, generate extended frameworks in mixed ligand systems, whereas the chelating terminal ligands, such as phen and 2,2'-bipy, often yield low-dimensional structures. The different

Thermogravimetric analysis

binding sites and conjugate skeletons provided by the auxiliary ligands have become the main factors influencing on the molecular structures and intramolecular interactions^{28, 29}.

To assess the thermal stability of complex **1**, thermogravimetric analysis was performed at a heating rate of 10 °C · min⁻¹ under nitrogen atmosphere. From the analysis of the thermal curve (Fig. 5), it appears that complex **1** is stable up to

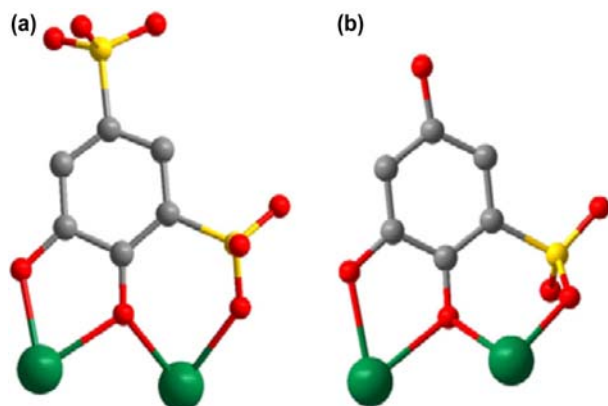


Fig. 4 — The coordination modes of (a) $\text{H}_2\text{Dhbds}^{2-}$ ligand and (b) $\text{H}_2\text{Thbs}^{2-}$ ligand

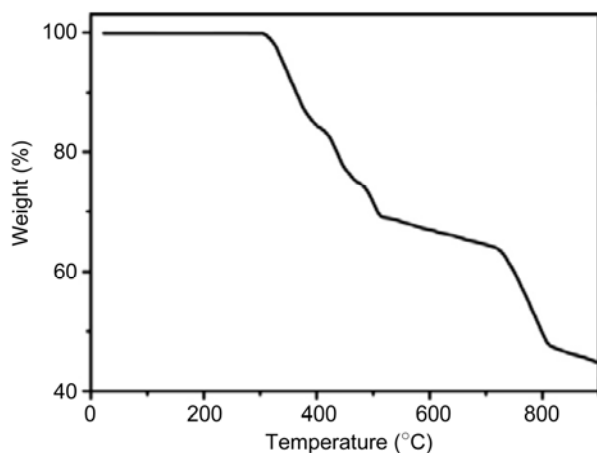


Fig. 5 — TGA curve for complex **1**

302 °C. On further heating, four phen molecules are decomposed in the temperature range of 302 °C-472 °C with the weight loss of 27.29% (calc. 27.50%). A continual weight loss occurs between 472 °C and 900 °C, which is attributed to the decomposition of $\text{H}_2\text{Dhbds}^{2-}$ and $\text{H}_2\text{Thbs}^{2-}$ ligands. However, it's not completely decomposed at 900 °C with the total weight loss of 78%.

Luminescence property

The solid state emission spectra of complex **1**, $\text{Na}_2\text{H}_2\text{Dhbds}$ and NaH_3Thbs under ambient temperature are measured with the same excitation wavelength of 380 nm. The emission spectra are shown in Fig. 6. The broad emission bands at 439 and 408 nm were observed for free $\text{Na}_2\text{H}_2\text{Dhbds}$ and NaH_3Thbs ligands, respectively. They may be originated from the $\pi-\pi^*$ intraligand charge transitions³⁰. Complex **1** displays the luminescence with a maximum band at 365 nm upon excitation at 380 nm. The emission profile of complex **1**

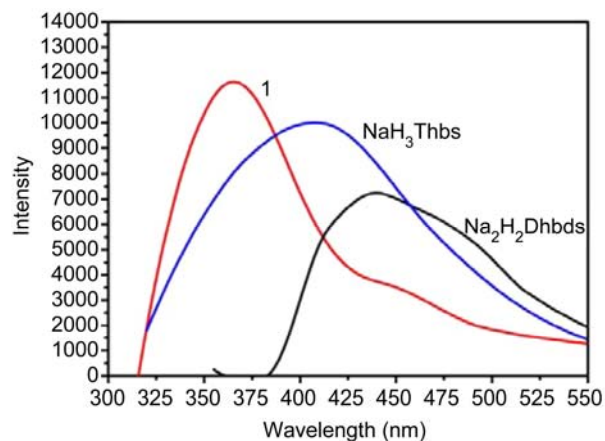


Fig. 6 — Solid-state emission spectra of complex **1**, $\text{Na}_2\text{H}_2\text{Dhbds}$ and NaH_3Thbs ligands at room temperature

is similar to those of free $\text{Na}_2\text{H}_2\text{Dhbds}$ and NaH_3Thbs ligands. So, it is attributable to the intraligand charge transitions, such as $\pi-\pi^*$ charge transitions³⁰. Complex **1** presented a relatively strong photoluminescence emission, which has the blue-shift of 74 nm and 43 nm in contrast to free $\text{Na}_2\text{H}_2\text{Dhbds}$ and NaH_3Thbs ligands, respectively. The blue shift is likely caused by the coordination of multi-functional ligands with Y ions and the $\pi-\pi$ interaction between phen molecules³¹.

Conclusions

In summary, a novel yttrium complex, $[\text{Y}_2(\text{H}_2\text{Dhbds})_3(\text{phen})_2] \cdot [\text{Y}_2(\text{H}_2\text{Dhbds})_2(\text{H}_2\text{Thbs})(\text{phen})_2]$, was successfully synthesized and structurally characterized. It features two dinuclear structural units bridged by $\text{H}_2\text{Dhbds}^{2-}$ and $\text{H}_2\text{Thbs}^{2-}$ ligands, with the Y...Y distances of 3.5267 Å and 3.5218 Å. Four yttrium atoms are eight-coordinated, and the arrangement around each yttrium atom is distorted double capped triangular prism. The phen molecules are engaged in the intermolecular $\pi-\pi$ stacking interactions, leading to the formation of a one-dimensional chain structure. Moreover, complex **1** exhibits the photoluminescence with the emission at 365 nm in the solid state, which is attributed to the intraligand charge transitions. Compared with free $\text{Na}_2\text{H}_2\text{Dhbds}$ and NaH_3Thbs ligands, complex **1** has the blue-shift of 74 nm and 43 nm, respectively, which is caused by the coordination and $\pi-\pi$ interaction.

Funding

Scientific Research Fund Project of Liaoning Provincial Education Department (No.L2019010).

Acknowledgement

We are thankful to Liaoning Province Education Department (No. L2019010) for financial support.

References

- 1 Angell S E, Rogers C W, Zhang Y, Wolf M O & Jones W E, *Coord Chem Rev*, 250 (2006) 1829.
- 2 Yasuchika H, *Bull Chem Soc Jap*, 87 (2014) 1029.
- 3 Ma Z B & Moulton B, *Coord Chem Rev*, 255 (2011) 1623.
- 4 Luo L, Lai P W, Wong K L, Wong W T, Li K F & Cheah K W. *Chem Phys Lett*, 398 (2004) 372.
- 5 Ejima H, Richardson J J, Liang K, Best J P, Koeverden M P V, Such G K, Cui J W & Caruso F, *Science*, 341 (2013) 154.
- 6 Girardot C, Lemerrier G, Mulatier J C, Chauvin J, Baldeck P L & Andraud C, *Dalton Trans*, (2007) 3421.
- 7 Wei G H, Yang J, Ma J F, Liu Y Y, Li S L & Zhang L P, *Dalton Trans*, (2008) 3080.
- 8 Yuan D, Li Y, Li W & Li S, *Phys Chem Chem Phys*, 20 (2018) 28894.
- 9 Liu Y, Liu L, Zhang X, Liang G & Gong X, *Acta Crystallogra*, 74 (2018) 13.
- 10 Li Q, Wu T, Lai J C, Fan Z L, Zhang W Q, Zhang G F, Cui D & Gao Z W, *Eur J Inorg Chem*, 2015 (2015) 5281.
- 11 Kaczmarek M T, Kubicki M & Radecka-Paryzek W, *Struct Chem*, 21 (2010) 779.
- 12 Indrani M, Ramasubramanian R, Fronczek F R, Vasanthacharya N Y & Kumaresan S, *J Mol Structure*, 931 (2009) 35.
- 13 Friese V A & Kurth D G, *Curr Opin Colloid In*, 14 (2009) 81.
- 14 Sun C, Xu L, An H, Li Y, Wang E & Xiao D, *Inorg Chem*, 44 (2005) 6062.
- 15 Kurc T, Janczak J, Hoffmann J & Videnova-Adrabsinska V, *Crystal Growth Des*, 12 (2012) 2613.
- 16 Wang Y L, Liu Q Y & Xu L, *Inorg Chem Commun*, 11 (2008) 851.
- 17 Jiang M X, Feng Y L, He Y H & Su H, *Inorg Chim Acta*, 362 (2009) 2856.
- 18 Hu B W, Zhao J P, Yang Q, Zhang X F & Bu X H, *Sci China Chem*, (2009) 1451.
- 19 Wang Y L & Xu Q Y L, *Cryst Eng Comm*, 10 (2008) 1667.
- 20 Shankar R, Jain A, Kociok-Köhn G & Molloy K C, *Inorg Chem*, 50 (2011) 1339.
- 21 Fu R, Hu S & Wu X, *Dalton Trans*, (2009) 9843.
- 22 Li F F, Ma J F, Song S Y, Yang J, Jia H Q & Hu N H, *Crystal Growth Des*, 6 (2006) 209.
- 23 Ma J F, Yang J, Li S L & Song S Y, *Crystal Growth Des*, 5 (2005) 807.
- 24 Sheldrick G M, *SHELXL-2018, Program for X-ray Crystal Structure Solution*, University of Göttingen, Göttingen, 2018.
- 25 Costes J P & Vendier L, *Eur J Inorg Chem*, 2010 (2010) 2768.
- 26 Efthymiou C G, Georgopoulou A N, Papatriantafyllopoulou C, Terzis A, Raptopoulou C P, Escuer A & Perlepes S P, *Dalton Trans*, 39 (2010) 8603.
- 27 Kani İ & Kurtça M, *Turkish J Chem*, 37 (2014) 993.
- 28 Song J, Li C R, Xu Q, Xu X T, Sun L X & Xing Y H, *Spectrochim Acta A*, 150 (2015) 308.
- 29 Cao H Y, Liu Q Y, Li L Q, Wang Y L, Chen L L & Yao Y, *Z Anorg Allg Chem*, 640 (2014) 1420.
- 30 Li X, Cao R, Bi W H, Yuan D Q & Sun D F, *Eur J Inorg Chem*, 2005 (2005) 3156.